International Journal of Innovative Technology and Exploring Engineering (IJITEE)
ISSN: 2278-3075 (Online), Volume-8 Issue-11, September 2019

Multi-Level Thresholding with Fractional-Order Darwinian PSO and Tsallis Function

R.Pugalenthi, A.Sheryl Oliver

Abstract*: *A novel optimal multi-level thresholding is proposed using gray scale images for Fractional-order Darwinian Particle Swarm Optimization (FDPSO) and Tsallis function. The maximization of Tsallis entropy is chosen as the Objective Function (OF) which monitors FDPSO's exploration until the search converges to an optimal solution. The proposed method is tested on six standard test images and compared with heuristic methods, such as Bat Algorithm (BA) and Firefly Algorithm (FA). The robustness of the proposed thresholding procedure was tested and validated on the considered image data set with Poisson Noise (PN) and Gaussian Noise (GN). The results obtained with this study verify that, FDPSO offers better image quality measures when compared with BA and FA algorithms. Wilcoxon's test was performed by Mean Structural Similarity Index (MSSIM), and the results prove that image segmentation is clear even in noisy dataset based on the statistical significance of the FDPSO with respect to BA and FA.

KEYWORDS:* *Image thresholding, Tsallis function, Fractional-order Darwinian PSO, Robustness analysis, Image quality measures, Wilcoxon's test.

I. INTRODUCTION

In image processing discipline, image segmentation is a necessary procedure to extract significant information from gray or color images in many fields, such as remote sensing [1-4], medicine [5-7] and pattern recognition [8]. The obtained digital image usually defined as an array of real or complex numbers which can be represented by a finite number of bits, further segmentation to be done by using traditional or modern computational techniques. Multi-level thresholding plays a major role in image segmentation, in which an image is separated into multiple regions or objects in order to find and interpret any meaningful information within the image.

A threshold (T) value is selected through a chosen signal processing scheme, and the highest intensity image pixels greater that T are considered as the first cluster, while the remaining lower intensity image pixels are chosen as a second cluster [9,10]. Determining the exact threshold (T) level to separate an image into desirable objects (foreground and background) remains an extremely complex and significant step in image segmentation. Comprehensive thresholding strategies are found in the literature [11-13].

Several researchers were identified and implemented considerable number of procedures, classified as parametric or nonparametric, and bi-level or multi-level thresholding on a class of images. Heuristic-based multi-thresholding approaches have been adopted to segment gray scale [14-18], RGB [19, 20] and multi-spectral images [1, 3, 4]. In the image thresholding literature, heuristic-based global thresholding methodologies, such as Otsu, Kapur, Renyi, Fuzzy and Shannon's entropy, are extensively discussed by researchers [11, 12].

In this proposed work, Tsallis entropy based global thresholding scheme was considered. Tsalis entropy is a non-extensive statistical approach [21-23], being typically adopted in image processing applications [24-31]. The combination of Tsallis function and heuristic algorithms, such as particle swarm optimization (PSO) [24-26], differential evolution [27-29], bacterial foraging [30], cuckoo search [31], and artificial bee colony [32,33], have been presented over the past years. Also Fractional-order Darwinian PSO (FDPSO) is use to segment the grayscale images with Tsallis function. A comparison was made side-by-side with Bat Algorithm (BA) and Firefly Algorithm (FA), using well-known image quality measures [34, 35].

The challenging work in medical imaging and remote sensing applications is getting a clear image as there are various irregularities in image capturing systems. These irregularities are caused by surrounding illumination, temperature, etc. [5, 6, 36].When there is a considerable noise level, it is necessary to preprocess the images using filters. When the noise is within an acceptable level, the filtering process can be avoided and the image can be directly processed using a chosen image processing methodology [36]. The image thresholding methodology works well on high quality images, but may sometime fails to offer decent results on noisy images. Hence, in this paper, the robustness of segmentation process is evaluated on standard test images with a presented Poisson Noise (PN) and Gaussian Noise (GN) to the images for various threshold levels. In addition, the FDPSO-based segmentation procedure is statistically compared with BA and FA using Wilcoxon's test for both clear and noisy images using MSSIM.

Manuscript published on 30 September 2019.
***Correspondence Author(s)**
R.Pugalenthi, Associate Professor,Department of CSE, St.Joseph's College of Engineering,Chennai,India..
A.Sheryl Oliver, Associate Professor,Department of CSE, St.Joseph's College of Engineering,Chennai,India..

II. TSALLIS FUNCTION

In general, the entropy is related with the measure of chaos within a system. Shannon initially considered the entropy to measure the ambiguity regarding the information content of the system [31, 32]. Shannon stated that, when a physical system is separated as two statistically free subsystems A and B, then the entropy value can be expressed as:

$$S(A+B)=S(A)+S(B) \quad (1)$$

Based on Shannon's theory, a non-extensive entropy concept was proposed by Tsallis [22, 23] and defined as:

$$S_q=\frac{1-\sum_{i=1}^{T}(p_i)^q}{q-1} \quad (2)$$

Where T is the system potentials and q is the entropic index [32, 33]. Eq. (2) will meet the Shannon's entropy when $q \to 1$.

The entropy value can be expressed with a pseudo additivity rule as:

$$S_q(A+B)=S_q(A)+S_q(B)+(1-q).S_q(A).S_q(B) \quad (3)$$

in such a way that Tsallis entropy can be considered to find the optimal thresholds of an image. Consider a given image with L gray levels in the range {0,1, ..., L-1},with probability distributions pi = p0, p1, ..., pL-1.Tsallis multi-level thresholding can then be expressed as: f(T)=[T1,T2, ... , Tk] = argmax

$$[S_q^A(T)+S_q^B(T)+...+S_q^K(T)+(1-q).S_q^A(T).S_q^B(T)...S_q^K(T)] \quad (4)$$

where

$$S_q^A(T)=\frac{1-\sum_{i=0}^{t_1-1}\left(\frac{Pi}{P^A}\right)^q}{q-1}, \quad P^A=\sum_{i=0}^{t_1-1}Pi$$

$$S_q^B(T)=\frac{1-\sum_{i=t_1}^{t_2-1}\left(\frac{Pi}{P^B}\right)^q}{q-1}, \quad P^B=\sum_{i=t_1}^{t_2-1}Pi$$

$$S_q^K(T)=\frac{1-\sum_{i=t_k}^{L-1}\left(\frac{Pi}{P^K}\right)^q}{q-1}, \quad P^K=\sum_{i=t_k}^{L_2-1}Pi$$

are subject to the following constraints:

$$\left|P^A+P^B\right|-1<S<1-\left|P^A-P^B\right|$$

$$\left|P^B+P^C\right|-1<S<1-\left|P^B-P^C\right|$$

$$\left|P^K+P^{L-1}\right|-1<S<1-\left|P^K-P^{L-1}\right|$$

During the multi-level thresholding process, the aim is to find the optimal threshold value T which maximizes the objective function f(T). In the proposed work, the threshold values are chosen as T ={2, 3, 4, 5}, thus the required probability values are PA, PB, PC, PD and PE. In this work, the maximization of function f(T), which deals with the segmentation of a given image, is carried using the FDPSO algorithm and compared with heuristic algorithms, namely BA and FA.

III. FRACTIONAL-ORDER DARWINIAN PARTICLE SWARM OPTIMIZATION

FDPSO integrates the concept of fractional calculus [37] which demonstrates a potential for interpreting evolution of the algorithm, with DPSO [38]. A detailed description of the FDPSO algorithm can be found in [39]. In the traditional PSO, the FDPSO is represented by difference equations describing the particles of motion. However, in the later, instead of a single swarm, there are several coopetitive swarms, striving to find the best solution to the problem [38]. As such, both velocity $v_n^s[t+1]$ and position $x_n^s[t+1]$ update of each particle n from swarm s at time/iteration t+1, can be first presented by Eq. (5) and Eq. (6) [40].

$$v_n[t+1]=wv_n[t]+\sum_{i=1}^{2}\rho_i R_i(x_{i_n}[t]-x_n[t]) \quad (5)$$

$$x_n[t+1]=x[t]+v_n[t+1] \quad (6)$$

Where in $x_{n_1}^s$ is the cognitive (local) best position of particle n and $x_{n_2}^s$ is the social (global) best position of its own swarm s. The other coefficients mainly weight these cognitive and social components, such that w is the inertial coefficient, ρ1 and ρ2 are the cognitive and social coefficients respectively, and r_i are random parameters uniformly distributed, which are necessary to provide stochasticity into the method.

Besides improving its traditional counterpart using multiple swarms, in FDPSO, the velocity update of the traditional PSO (Eq.5) is enhanced using fractional calculus. To that end, let us first define the approximate discrete time Grünwald–Letnikov fractional difference of order α, $\alpha \in \mathbb{C}$, of a generic discrete signal x(t)as [2, 37, 39]:

$$D^\alpha[x[t]]=\frac{1}{T_s^\alpha}\sum_{k=0}^{r}\frac{(-1)^k\Gamma[\alpha+1]x[t-kT_s]}{\Gamma[k+1]\Gamma[\alpha-k+1]} \quad (7)$$

where Ts is the sampling period and r is the truncation order.

For a specific swarm s and by considering the inertial co-efficient $w=1$, Eq. 5 can be rewritten as:

$$v_n^s[t+1]-v_n^s[t]=\sum_{i=1}^{2}\rho_i R_i(x_{i_n}^s[t]-x_n^s[t]) \quad (8)$$

Equation (8) is the discrete version of the fractional difference in order $\alpha=1$. For a unitary sampling time, Ts = 1, Eq. 8 can then be rewritten as:

$$D^\alpha[v_n^s[t+1]]=\sum_{i=1}^{2}\rho_i R_i(x_{i_n}^s[t]-x_n^s[t]) \quad (9)$$

which yields

Published By:
Blue Eyes Intelligence Engineering
and Sciences Publication (BEIESP)

$$v_n^s[t+1] = -\sum_{k=1}^{r} \frac{(-1)^k \Gamma[\alpha+1] x[t-kT_s]}{\Gamma[k+1]\Gamma[\alpha-k+1]} + \sum_{i=1}^{2} \rho_i R_i (x_{in}^s[t] - x_n^s[t]) \quad (10)$$

The above equation (10) represents the velocity update of the FDPSO, which basically considers a short-term memory effect due to the truncation order r. contrarily to other stochastic alternatives, which are memory less, particles motion within the FDPSO is affected by the previous r iterations that may comprise multiple solutions.

FDPSO is a natural generalization of the DPSO in which the particles are unable to improve for a certain number of iterations that are deleted, while particles that are able to constantly find ever-improving solutions are rewarded with more collaborative particles [38].

To overcome the complex problems, FDPSO is adopted that provides a high immunity to sub-optimal (local) solutions by using Rastrigin function [39], or even time-variant functions [41].

3.1 OTHER HEURISTIC ALGORITHMS IN THIS STUDY

In order to validate the performance of the FDPSO algorithm, recent heuristic algorithms, such as the Bat Algorithm (BA) and the Firefly Algorithm (FA), are considered. A detailed explanation about BA are found in [14, 17, 42-44] and FA are found in [18, 20, 42, 45, 46]. Table 1 represents the initial algorithm parameters for FDPSO,BA and FA for image segmentation proces

Table1. Initial parameters of heuristic algorithms

Parameter	FDPSO	BA	FA
No. of Iterations	1000		
Search dimension d	No. of thresholds (T) = 2 to 5		
Candidate population	d×10		
Maximum agents' position X_{max}	255		
Minimum agents' position X_{min}	0		
Run length for the heuristic search (Iterations)	1000		
Stopping criteria	J_{max}		
Algorithm specific parameters	Min population = d×5; Max population = d×12; Number of swarms = d×2; Min swarms = d; Max swarms = d×3; Stagnancy = d×5	β = [0,1];which is the Frequency vector constant ε ranges from [-1,1]; which is a random value $\alpha^1 = \gamma^1$=0.75 is set in which A_0 = 10 and A_{min}= 1 (decays in steps of 0.1);	γ = 5,Light absorption co-efficient the attractiveness β_0 = 1 Randomization parameter $\psi = \alpha' \varepsilon_i$ (α' = randomization operator ε_i = random variable drawn from a Gaussian distribution)

IV. IMPLEMENTATION

In grayscale level images, multi-level thresholding deals with finding the most favorable thresholds within the range [0, L-1] that maximize a considered fitness criterion. In the proposed paper, multi-level segmentation has been fulfilled by employing an unsupervised nonparametric approach with heuristic algorithms.

As depicted in section 2, the Tsallis function may be considered as an important metric segmentation operation, in which the q (entropic index) value needs to be assigned properly so as to get an improved solution. The literature offers different choices of q, such as $q < 1$ which represents the sub-extensive entropy, q =1 which represents the extensive entropy, and $q > 1$ which represents the super-extensive entropy [31, 32]. In this experimental study, q was chosen to be 4, while q = 1, be the super-extensive entropy offers an improved segmentation performance when compared with other entropic index values [31].

Initially, the optimization search was carried out with various candidate sizes, such as 10, 20, 30, 40 and 50, for T=2, and it was possible to observe that a maximum of 10 candidates is sufficient to find the solution. It is noteworthy that if larger candidate size is chosen, the CPU run time would significantly increase with respect to the candidate size in order to achieve a similar $f(T)$. This analysis confirms that the objective function $f(T)$ mainly depends on the chosen T. Hence, in this work, the candidate population is chosen as d×10, as presented in Table 1.

In heuristic algorithms, each candidate solution represents a set of T threshold values which will result in a different $f(T)$. During the initialization, a population of solutions is randomly generated within the range [0, L-1] for each dimension. After generating the population, solutions within the population are assigned with a fitness value. The algorithm starts to explore the search space until it finds the optimal thresholds which maximize the fitness function $f(T)$.

The implementation of the multi-thresholding scheme is described as it follows:

Step1: Initialize the FODPSO algorithms with nominal parameters as depicted in Table 1. Assign the required threshold value (dimension of search'd').

Step 2: Plot the histogram of the image. Initialize particles at random locations

Step 3: Using particles position, arbitrarily choose the threshold (T) values and Compute *f* (T). Adjust both position and velocity of particles towards the optimal fitness value by following equations (6) and (10). Iteratively repeat the procedure until *f* (T) attains a maximized value, or the iteration reaches the utmost value.

Step 4: Move the entire population towards the optimal f(T)

Step 5: If the search reaches an optimal *f* (T). Stop the search and display the value of *f* (T), optimal threshold, search pattern and segmented image. Else, repeat from Step 2.

Step 6: Compute the image quality measures and record the optimal values

Step 7: Repeat the segmentation procedure with a new threshold (T) value.

4.1 Image Quality Measures

The quality of the segmented images in this paper is assessed with well-known image metrics, namely the Peak Signal-to-Noise Ratio (PSNR), Mean Structural Similarity Index (MSSIM) [34], Tsallis fitness function value and CPU time (in seconds). Additionally, image quality measures, such as Normalized Absolute Error (NAE), Normalized Cross-Correlation (NCC), Average Difference (AD) and Structural Content (SC) are also considered [35]. Along with the above said quality measures, the Standard Deviation (STD) for each variable is also computed to assess the stability of the heuristic search [2, 9, 10].

Higher values of PSNR, MSSIM, NCC and lower values of NAE, AD, and SC specify a superior quality of thresholding. An improved Tsallis fitness function with minor CPU time during the optimization search also confirms the superior performance of the heuristic algorithm.

4.2 Robustness Analysis

The robustness of the proposed segmentation procedure is additionally assessed using test images with noise. During real-time image processing situations, the image captured with an imaging device may be corrupted with noise due to various reasons, such as improper illumination, surrounding temperature changes, faults in electronic circuits, etc. Hence, it is necessary to analyze the healthiness of the image segmentation scheme. In this work, the robustness of the proposed segmentation process is confirmed with the image data set stained with Salt and Pepper Noise (SPN), Poisson Noise (PN), Speckle Noise (SN) and Gaussian Noise (GN). The results revealed that the proposed FDPSO based multi-thresholding offers better results when compared with the other alternatives. Furthermore, the statistical significance of the proposed scheme is proved using a non-parametric approach known as Wilcoxon's rank test [47, 48]. In this test, the pair wise assessment of MSSIM is done as FDPSO vs. BA and FDPSO vs. FA for clear and noisy test images. The novel FDPSO based optimal multi thresholding offers very good image segmentation for clear and noisy test images.

V. RESULTS AND DISCUSSIONS

All experiments are carried out on a computer with AMD C70 Dual Core 1 GHz CPU, 4GB of RAM and Matlab R2010a software. For statistical purposes, the thresholding process is repeated 40 times for each image with a chosen *T* value and the mean value (mean ± STD) among the trials is recorded as the optimal value. The proposed multi-thresholding procedure is implemented on 481 × 321 sized gray scale images available at Berkeley image database [49].

5.1 Images Without Noise

In this work, the grayscale images, such as butterfly, starfish, snake, jet, desert and pyramid are considered and are presented in Table 2. In the gray histogram, the *x*-axis represents the gray level and the *y*-axis denotes the pixel level.

Initially, multi-thresholding is executed with the butterfly image for T= {2, 3, 4, 5}. The convergence of the heuristic search towards an optimal f(T) is presented in Fig. 1 and the corresponding performance measure values, such as CPU time, STD, PSNR, MSSIM, NAE, NCC, AD and SC are presented in Table 3 and Table 5. Table 4 presents the segmented image for T= {2, 3, 4, 5} and the corresponding threshold values achieved using the FDPSO algorithm and maximized f(T) is available in Table 13 in this, highlighted contents shows the better values. Table 13 also presents the SSIM map of the segmented Butterfly image for T= {2, 3, 4, 5}. This segmentation procedure is extended for the remaining images in the considered dataset and the corresponding image quality measures are registered.

As one may observe through the example in Fig. 1, the FDPSO does not always present the best convergence rate. Yet, in all the occasions on an average, and as depicted in the

Table 2. Chosen test images (481 x 321) and corresponding gray histogram

	Original image	Histogram		Original image	Histogram
Butterfly		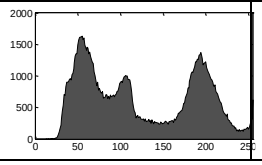	Jet		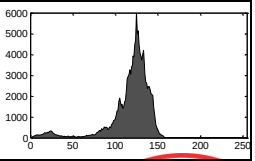

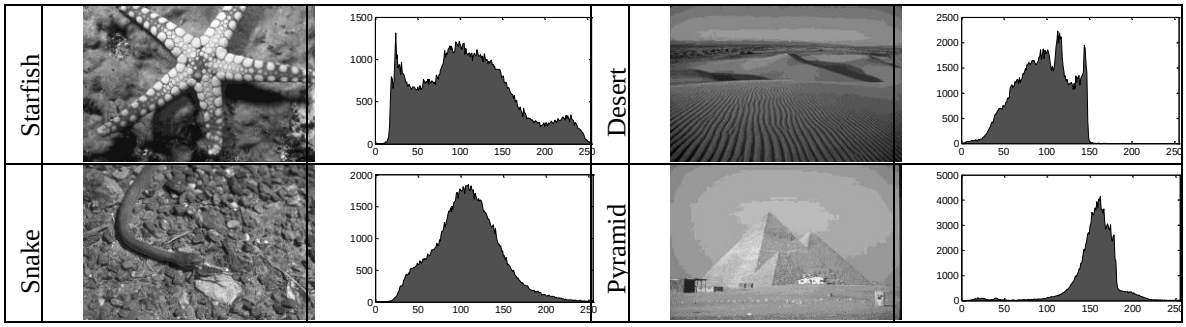

following tables, it is the one that presents the most superior overall performance for clear and noisy image cases, when compared with BA and FA.

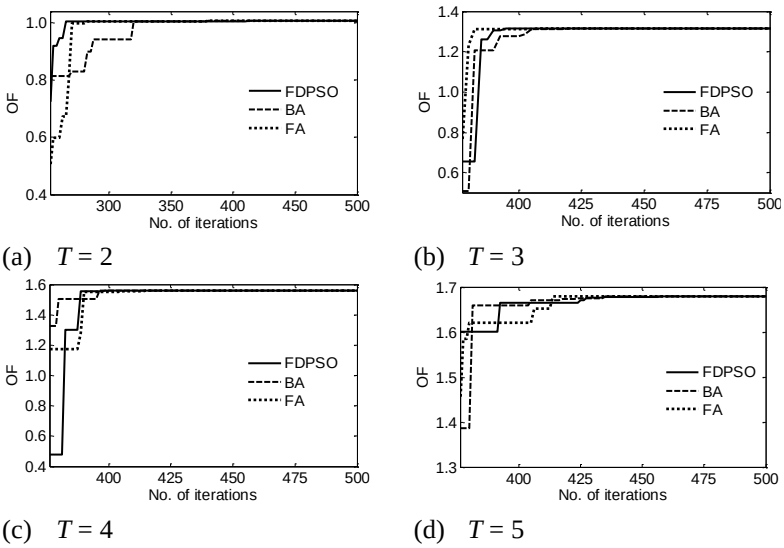

(a) $T = 2$ (b) $T = 3$

(c) $T = 4$ (d) $T = 5$

Fig. 1 Convergence of optimization search for Butterfly image

Table 3. Comparison of CPU time, PSNR and MSSIM

	T	CPU time (s)			PSNR(dB)			MSSIM		
		FDPSO	BA	FA	FDPSO	BA	FA	FDPSO	BA	FA
Butterfly	2	10.24±0.32	**9.82±0.27**	11.25±0.29	**12.74±0.05**	11.44±0.11	11.50±0.03	**0.49±0.01**	0.43±0.08	0.47±0.15
	3	**11.68 ±0.12**	13.17± 0.36	12.89±0.16	**13.17±0.02**	12.32±0.06	12.41±0.02	**0.54±0.01**	0.49±0.06	0.51±0.09
	4	17.38 ±0.32	20.62± 0.40	**16.18±0.29**	**14.48±0.01**	13.18±0.27	14.02±0.10	**0.62±0.04**	0.59±0.10	0.58±0.06
	5	**26.62 ±0.25**	28.83± 0.33	28.10±0.28	**15.93±0.01**	13.79±0.10	14.41±0.05	**0.65±0.01**	0.64±0.01	0.64±0.14
Starfish	2	**8.12 ±0.08**	9.16± 0.12	8.84±0.10	**11.27±0.02**	10.16±0.11	10.25±0.07	**0.45±0.01**	0.43±0.12	0.41±0.08
	3	13.38 ±0.04	13.14± 0.16	**12.91±0.02**	**14.62±0.02**	10.71±0.07	10.75±0.10	**0.48±0.02**	0.44±0.02	0.44±0.04
	4	19.46 ±0.28	20.30± 0.40	**19.08±0.11**	**15.22±0.01**	12.85±0.11	12.61±0.08	**0.61±0.02**	0.57±0.02	0.57±0.06
	5	**31.92 ±0.32**	32.58± 0.38	32.14±0.36	**16.36±0.01**	15.13±0.11	14.84±0.03	**0.69±0.01**	0.60±0.08	0.59±0.02
Snake	2	**9.26 ± 0.17**	11.10± 0.22	10.77±0.21	**10.10±0.08**	8.38±0.10	8.56±0.14	**0.45±0.01**	0.41±0.03	0.42±0.01
	3	**12.06 ±0.22**	14.63± 0.28	13.58±0.28	**11.75±0.01**	9.33±0.03	9.37±0.05	**0.49±0.03**	0.42±0.05	0.44±0.15
	4	19.04 ±0.21	**18.16± 0.26**	18.22±0.27	**13.38±0.02**	12.45±0.08	12.84±0.09	**0.57±0.01**	0.54±0.18	0.56±0.02
	5	**27.11 ±0.12**	27.39± 0.14	27.24±0.18	**15.97±0.01**	14.48±0.05	14.74±0.03	**0.67±0.01**	0.63±0.05	0.63±0.01
Jet	2	12.83 ±0.16	13.86± 0.20	**12.08±0.08**	**8.15±0.01**	6.75±0.03	6.93±0.06	**0.72±0.01**	0.67±0.12	0.69±0.03
	3	**13.62 ±0.13**	14.93± 0.17	14.14±0.19	**11.13±0.01**	9.84±0.02	10.17±0.03	**0.79±0.01**	0.74±0.09	0.72±0.17
	4	19.75 ±0.20	19.38± 0.32	**19.05±0.14**	**14.88±0.04**	12.66±0.09	12.72±0.08	**0.80±0.05**	0.78±0.11	0.77±0.13
	5	**32.18 ±0.11**	33.71± 0.16	32.75±0.23	**15.54±0.01**	13.46±0.11	13.36±0.05	**0.81±0.01**	0.80±0.02	0.80±0.01
Desert	2	**12.54 ±0.05**	13.42± 0.10	13.18±0.15	**8.16±0.01**	5.64±0.06	5.35±0.07	**0.48±0.01**	0.46±0.26	0.47±0.05
	3	**15.33 ±0.08**	**15.33± 0.10**	18.26±0.12	**8.95±0.01**	5.92±0.03	6.12±0.02	**0.56±0.01**	0.52±0.07	0.54±0.06
	4	22.16 ±0.11	21.28± 0.19	**21.19±0.05**	**10.84±0.07**	7.44±0.16	7.69±0.10	**0.59±0.01**	0.57±0.02	0.58±0.11
	5	**28.93 ±0.12**	32.42± 0.18	32.00±0.27	**11.15±0.01**	7.98±0.07	7.91±0.02	**0.61±0.01**	0.59±0.12	0.61±0.08

Pyramid	2	**9.54 ± 0.03**	10.18± 0.08	9.83±0.10	**14.91±0.02**	14.45±0.03	14.14±0.0	**0.69±0.01**	0.58±0.06	0.63±0.05
	3	14.97 ±0.30	13.55± 0.38	**13.08±0.25**	**15.26±0.01**	14.70±0.02	14.84±0.01	**0.75±0.01**	0.70±0.18	0.70±0.02
	4	**17.42 ±0.15**	20.03± 0.24	20.51±0.18	**16.49±0.02**	15.52±0.07	15.91±0.03	**0.77±0.02**	0.75±0.02	0.76±0.02
	5	**24.06 ±0.04**	28.18± 0.16	28.34±0.14	**21.58±0.01**	18.90±0.07	20.38±0.05	**0.79±0.01**	0.77±0.14	0.78±0.05
Average		**17.90 ±0.16**	18.97±0.23	18.57±0.19	**13.42±0.02**	11.56±0.08	11.74±0.05	**0.63±0.02**	0.59±0.08	0.60±0.07

Table 4. Thresholded images and corresponding threshold values

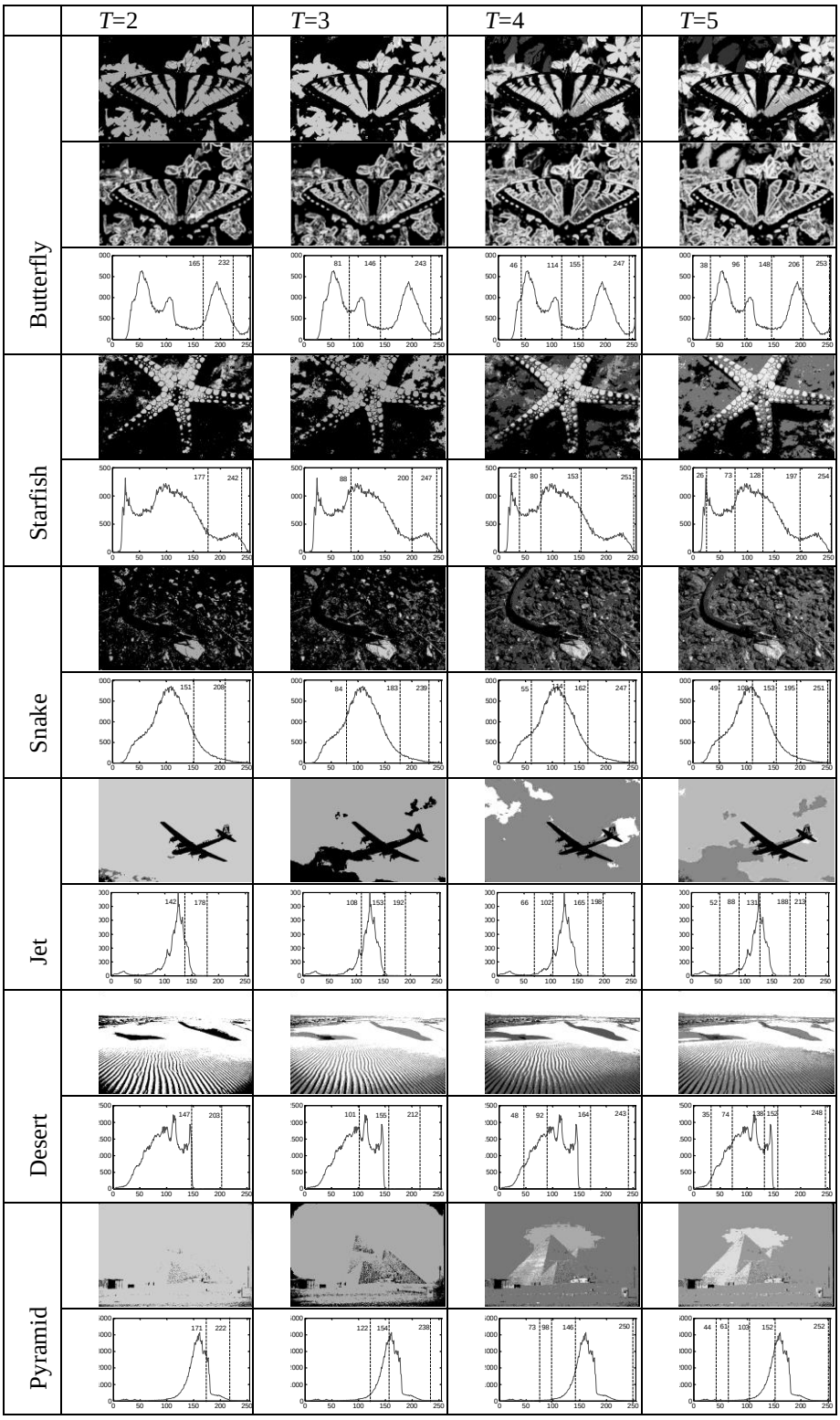

Table 5. Image quality measure values

	T	NAE			NCC			AD			SC		
		FDPSO	BA	FA	FDPSO	BA	FA	FDPSO	BA	FA	FDPSO	BA	FA
Butterfly	2	**0.43±0.08**	0.47±0.09	0.45±0.11	**0.68±0.04**	0.66±0.10	0.65±0.07	**56.64±0.15**	61.39±0.21	58.15±0.16	**1.54±0.01**	1.74±0.02	1.68±0.01
	3	**0.40±0.04**	0.42±0.10	0.42±0.04	**0.85±0.02**	0.78±0.05	0.82±0.02	**40.85±0.18**	54.82±0.16	42.93±0.10	**1.28±0.02**	1.51±0.15	1.40±0.02
	4	**0.34±0.02**	0.38±0.06	0.35±0.03	**0.87±0.01**	0.83±0.03	0.85±0.02	**33.85±0.21**	42.19±0.30	37.19±0.18	**1.07±0.03**	1.13±0.04	1.19±0.08
	5	**0.33±0.05**	0.34±0.07	0.33±0.09	**0.89±0.07**	0.86±0.05	0.88±0.12	**26.38±0.12**	36.63±0.15	31.04±0.11	**1.01±0.02**	1.07±0.06	1.14±0.05
Starfish	2	**0.62±0.04**	0.64±0.08	0.63±0.08	**0.57±0.03**	0.51±0.11	0.54±0.02	**56.76±0.17**	59.39±0.19	63.10±0.18	**1.81±0.05**	1.85±0.15	1.85±0.12
	3	**0.51±0.01**	0.56±0.02	0.58±0.05	**0.63±0.08**	0.58±0.24	0.60±0.08	**51.03±0.01**	56.18±0.10	52.99±0.05	**1.54±0.02**	1.74±0.10	1.61±0.03
	4	**0.42±0.03**	0.51±0.03	0.52±0.07	**0.73±0.02**	0.66±0.02	0.71±0.02	**43.24±0.05**	50.57±0.10	45.76±0.10	**1.56±0.01**	1.71±0.02	1.58±0.02
	5	**0.29±0.02**	0.38±0.03	0.41±0.02	**0.86±0.03**	0.71±0.03	0.84±0.02	**22.81±0.11**	29.02±0.12	23.94±0.10	**1.20±0.02**	1.43±0.15	1.36±0.10
Snake	2	**0.81±0.02**	0.88±0.10	0.86±0.06	**0.34±0.01**	0.31±0.02	0.29±0.02	**83.35±0.10**	87.27±0.16	85.39±0.10	**2.68±0.02**	2.95±0.01	4.06±0.01
	3	**0.72±0.07**	0.74±0.09	0.73±0.25	**0.38±0.01**	0.36±0.02	0.35±0.02	**76.24±0.10**	78.15±0.28	77.18±0.10	**2.26±0.02**	2.63±0.10	3.82±0.02
	4	**0.49±0.07**	0.61±0.06	0.58±0.08	**0.59±0.01**	0.48±0.02	0.49±0.02	**51.87±0.16**	52.18±0.19	63.50±0.25	**2.08±0.10**	2.51±0.10	3.20±0.02
	5	**0.33±0.03**	0.46±0.03	0.41±0.04	**0.74±0.01**	0.65±0.02	0.64±0.06	**34.95±0.12**	38.19±0.23	41.84±0.13	**1.65±0.02**	2.02±0.04	2.49±0.10
Jet	2	**0.82±0.02**	0.88±0.05	0.86±0.02	**0.42±0.01**	0.38±0.01	0.40±0.02	**51.99±0.04**	64.22±0.10	51.49±0.10	**0.77±0.01**	1.46±0.01	1.04±0.02
	3	**0.62±0.01**	0.70±0.09	0.69±0.01	**0.51±0.01**	0.47±0.01	0.50±0.02	**20.18±0.10**	42.05±0.10	36.08±0.10	**0.62±0.01**	1.19±0.01	0.82±0.12
	4	**0.48±0.03**	0.58±0.02	0.55±0.08	**0.66±0.05**	0.61±0.03	0.65±0.15	**18.29±0.08**	30.18±0.10	23.91±0.10	**0.59±0.01**	0.93±0.01	0.64±0.02
	5	**0.46±0.01**	0.52±0.06	0.51±0.10	**0.69±0.02**	0.66±0.04	0.67±0.02	**17.04±0.12**	26.66±0.15	20.05±0.10	**0.47±0.10**	0.58±0.10	0.55±0.04
Desert	2	**0.85±0.05**	0.88±0.11	0.86±0.07	**0.28±0.02**	0.25±0.02	0.27±0.02	**61.37±0.11**	68.18±0.17	63.22±0.17	**4.18±0.05**	4.41±0.05	4.49±0.07
	3	**0.80±0.02**	0.82±0.03	0.81±0.03	**0.34±0.01**	0.32±0.01	0.33±0.05	**58.95±0.05**	60.67±0.10	59.56±0.10	**3.74±0.02**	4.27±0.04	3.95±0.12
	4	**0.73±0.01**	0.77±0.01	0.74±0.04	**0.46±0.01**	0.42±0.03	0.40±0.02	**51.39±0.11**	57.02±0.10	53.28±0.10	**3.40±0.02**	4.04±0.10	3.86±0.10
	5	**0.71±0.05**	0.74±0.06	0.72±0.11	**0.58±0.01**	0.43±0.02	0.42±0.10	**46.74±0.18**	54.15±0.22	51.04±0.16	**3.16±0.02**	3.75±0.15	3.61±0.10
Pyramid	2	**0.47±0.03**	0.58±0.03	0.51±0.05	**0.48±0.02**	0.41±0.02	0.46±0.06	**55.32±0.04**	57.18±0.10	62.19±0.10	**2.29±0.08**	3.63±0.11	2.84±0.01
	3	**0.36±0.02**	0.51±0.05	0.46±0.02	**0.56±0.01**	0.49±0.02	0.53±0.02	**36.20±0.02**	55.93±0.07	49.88±0.10	**2.05±0.04**	3.27±0.10	2.22±0.02
	4	**0.23±0.02**	0.45±0.03	0.38±0.02	**0.80±0.01**	0.68±0.02	0.74±0.02	**14.18±0.17**	21.10±0.22	32.19±0.20	**1.63±0.02**	3.02±0.05	2.08±0.01
	5	**0.11±0.02**	0.36±0.02	0.30±0.06	**0.97±0.01**	0.81±0.07	0.91±0.02	**4.81±0.03**	18.28±0.05	20.84±0.10	**1.04±0.01**	2.49±0.02	1.64±0.07
Average		**0.51±0.03**	0.59±0.06	0.57±0.06	**0.62±0.02**	0.56±0.04	0.58±0.04	**42.27±0.11**	50.07±0.15	47.78±0.12	**1.82±0.03**	2.31±0.07	2.21±0.05

From Table 5, the FDPSO utterly surpasses the alternatives in all situations, regardless on the number of thresholds *T*. Nevertheless, both BA and FA are sometimes able to achieve almost similar solutions, especially when the number of thresholds *T* is small (2 or 3). It is, therefore, necessary to further evaluate the FDPSO and compare it with the alternatives under more realistic experiments.

5.2 Images With Noise

The proposed image segmentation approach is then tested on the image dataset corrupted with various noises, such as SPN, PN, SN and GN. The noise level is chosen as follows:

- SPN : with a noise density of 0.05,
- PN : pixel dependent Poisson distribution with mean 10,
- SN : uniformly distributed random noise with mean 0 and variance 0.05
- GN : white noise of mean 0 and variance 0.01

Table 6 shows the gray scale histogram and computed PSNR values of noise stained test images. As an example, various noise corrupted Butterfly images are presented in the first row of Table 6, and similar results are obtained with other images. By observing Table 6, it is evident that there is a considerable impact on the histogram quality and the PSNR value of the image depending on the added noise. It can also be observed that the image pixel level degrades due to noise, and the histogram becomes smoother when compared with the original histogram (Table 2). Fig. 2 graphically depicts the changes in PNSR value with respect to the noise. Even though the PSNR value of SPN noise stained image is small when compared with other images, the histogram pattern imitates the original image. For other noise values, the histogram pattern degrades considerably. Hence, in this paper, an analysis is presented by considering PN and GN corrupted image dataset.

Table 6. Gray histogram and PSNR values of noise stained test images

	Salt & Pepper	Poisson	Speckle	Gaussian
Butterfly	 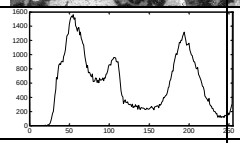	 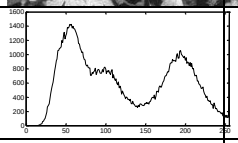	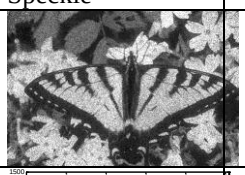 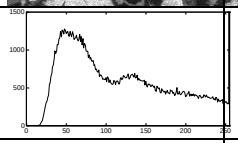	 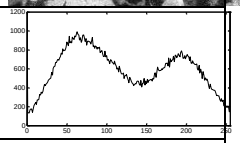
	17.9377	27.4088	18.5692	19.6675
Starfish	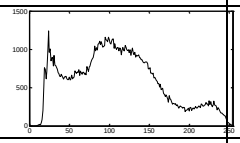	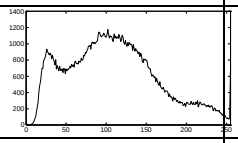	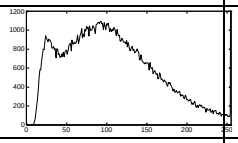	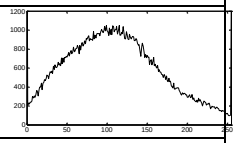
	18.0930	28.0469	19.4501	19.7081
Snake	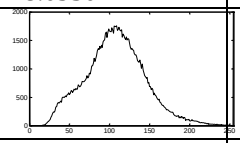	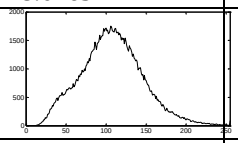	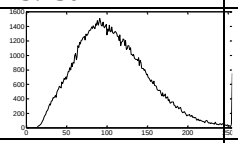	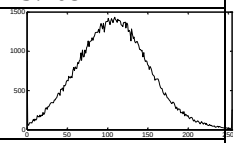
	18.4581	28.1552	19.5511	19.5350
Jet	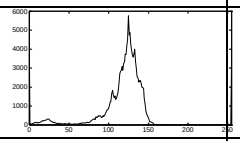	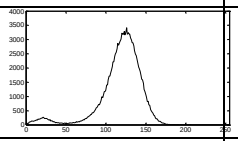	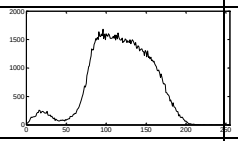	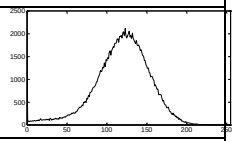
	18.6444	27.6312	19.0431	19.5175
Desert	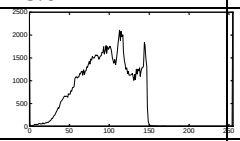	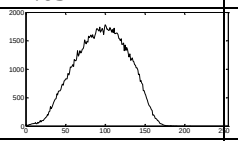	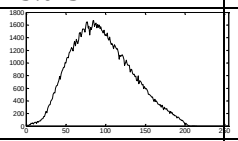	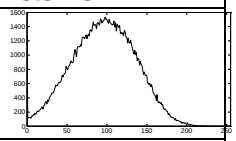
	18.3233	28.8225	20.5689	19.5275
Pyramid	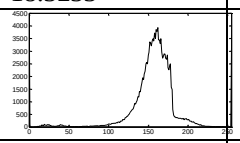	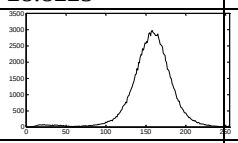	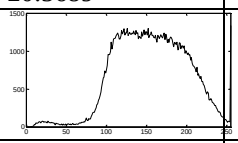	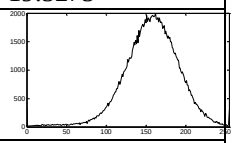
	18.5123	25.9947	16.9264	19.4843

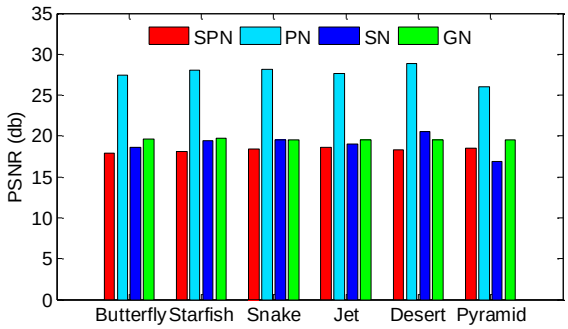

Fig. 2 PSNR value of noise corrupted test images

The multi-level thresholding process is then repeated on the chosen noisy image dataset and the results are presented in Table 7 -12.Table 8 presents the segmented image for *T*= {2, 3, 4, 5} and the corresponding threshold values obtained with FDPSO for PN stained images and Table 7,9 and Table 13 presents the comparison of performance measures obtained with FDPSO, BA and FA. From these tables, it can be noted that, the proposed FDPSO offers most superior f(T), PSNR, MSSIM, NAE, NCC, AD and SC compared with BA and FA for all the test cases. Similar results are obtained for GN stained images as depicted in Table 11-13. Table 10 presented the segmented test images and the corresponding optimal thresholds for various *T* values.

Table 7. Comparison of CPU time, PSNR and MSSIM for PN stained image

	T	CPU time (s)			PSNR(dB)			MSSIM		
		FDPSO	BA	FA	FDPSO	BA	FA	FDPSO	BA	FA
Butterfly	2	9.16±0.18	9.36±0.12	**8.46±0.16**	**15.04±0.01**	14.93±0.02	15.00±0.02	**0.39±0.01**	0.37±0.02	0.38±0.02
	3	12.79±0.06	14.17±0.10	**12.62±0.10**	**17.30±0.01**	16.20±0.02	16.97±0.02	**0.52±0.01**	0.51±0.01	0.51±0.01
	4	**18.56±0.10**	20.62±0.10	19.15±0.08	**20.26±0.02**	17.12±0.02	19.34±0.02	**0.63±0.01**	0.59±0.01	0.61±0.08
	5	**22.07±0.02**	25.11±0.10	23.16±0.05	**21.74±0.10**	19.00±0.11	20.00±0.02	**0.73±0.01**	0.68±0.01	0.69±0.11
Starfish	2	8.58±0.01	9.47±0.02	**8.43±0.02**	**17.07±0.05**	15.37±0.02	16.39±0.10	**0.35±0.01**	0.35±0.01	0.38±0.01
	3	**13.74±0.16**	14.73±0.15	14.02±0.04	**18.24±0.12**	16.11±0.08	17.16±0.12	**0.49±0.01**	0.41±0.02	0.46±0.01
	4	21.18±0.05	**20.06±0.10**	20.75±0.10	**19.88±0.01**	16.97±0.05	19.00±0.05	**0.59±0.01**	0.55±0.01	0.57±0.02
	5	**26.85±0.10**	29.15±0.10	27.47±0.11	**22.63±0.02**	18.16±0.10	20.18±0.01	**0.69±0.01**	0.67±0.01	0.69±0.01
Snake	2	10.55±0.10	**10.29±0.10**	11.05±0.08	**17.02±0.02**	15.94±0.08	16.94±0.03	**0.43±0.01**	0.40±0.02	0.42±0.01
	3	**14.02±0.02**	16.14±0.05	14.76±0.05	**17.84±0.01**	16.11±0.02	17.13±0.01	**0.57±0.01**	0.54±0.02	0.54±0.01
	4	**16.75±0.02**	19.86±0.02	17.14±0.02	**18.96±0.01**	17.38±0.02	17.96±0.01	**0.68±0.05**	0.65±0.01	0.68±0.10
	5	**22.16±0.02**	22.49±0.02	22.83±0.05	**22.77±0.01**	20.00±0.02	19.36±0.02	**0.79±0.02**	0.79±0.08	0.79±0.10
Jet	2	10.06±0.15	**9.47±0.10**	10.32±0.20	**18.87±0.05**	16.36±0.11	17.12±0.02	**0.37±0.01**	0.36±0.01	0.36±0.01
	3	**11.28±0.08**	11.84±0.10	12.25±0.10	**20.00±0.01**	18.16±0.05	19.00±0.02	**0.47±0.01**	0.46±0.01	0.46±0.02
	4	**16.92±0.11**	17.05±0.12	17.40±0.14	**20.78±0.02**	18.93±0.03	20.17±0.02	**0.50±0.01**	0.48±0.02	0.50±0.01
	5	21.46±0.10	22.36±0.12	**21.07±0.08**	**21.08±0.04**	19.11±0.01	20.90±0.10	**0.57±0.01**	0.54±0.01	0.56±0.01
Desert	2	**8.57±0.10**	9.04±0.15	9.28±0.11	**17.95±0.02**	17.18±0.02	16.94±0.11	**0.30±0.02**	0.29±0.01	0.30±0.05
	3	**12.42±0.01**	13.28±0.08	12.64±0.02	**19.79±0.01**	18.80±0.01	17.12±0.02	**0.44±0.02**	0.41±0.02	0.43±0.02
	4	18.86±0.02	18.93±0.05	**18.50±0.07**	**20.12±0.03**	19.83±0.07	19.64±0.02	**0.52±0.01**	0.51±0.01	0.51±0.03
	5	**21.09±0.10**	21.75±0.14	22.04±0.12	**22.00±0.02**	20.79±0.02	20.81±0.02	**0.61±0.01**	0.59±0.10	0.60±0.01
Pyramid	2	**6.24±0.11**	9.11±0.11	7.38±0.11	**18.16±0.01**	17.99±0.02	18.00±0.02	**0.34±0.01**	0.34±0.03	0.34±0.01
	3	**10.14±0.13**	12.26±0.15	12.29±0.11	**19.16±0.10**	18.40±0.11	18.86±0.12	**0.46±0.01**	0.43±0.01	0.44±0.01
	4	15.27±0.05	15.74±0.10	**14.46±0.10**	**21.10±0.05**	20.19±0.10	19.57±0.02	**0.57±0.01**	0.54±0.10	0.56±0.02
	5	**17.84±0.12**	18.04±0.12	18.84±0.10	**21.86±0.01**	20.79±0.02	20.45±0.02	**0.67±0.02**	0.67±0.05	0.65±0.10
Average		**15.27±0.08**	16.26±0.10	15.68±0.09	**19.57±0.03**	17.91±0.05	18.50±0.04	**0.53±0.01**	0.51±0.03	0.52±0.03

Table 8. Thresholded images and optimal threshold values (PN stained image)

	T=2	*T*=3	*T*=4	*T*=5
Butterfly		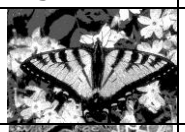		
	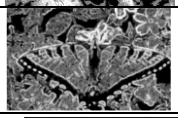			
	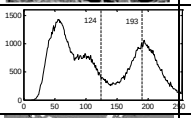	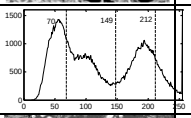	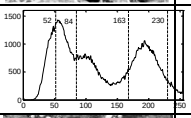	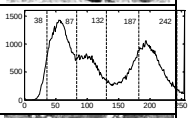
Starfish	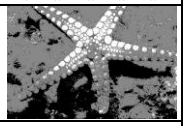	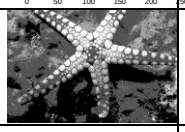	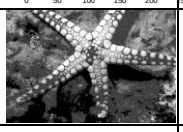	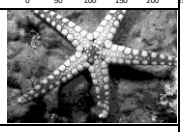
	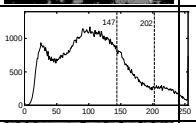	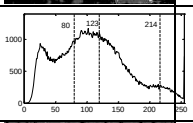	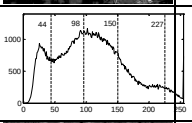	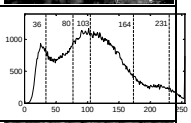
Snake	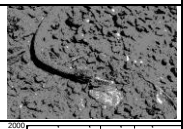			
	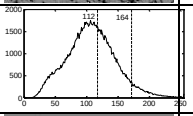	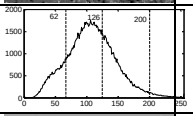	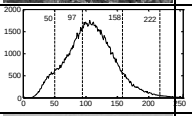	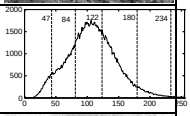
Jet				
	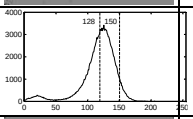	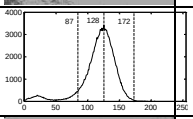	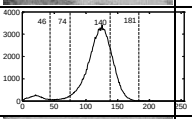	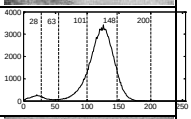
Desert	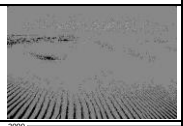	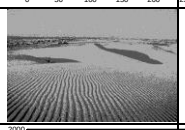		
	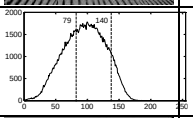	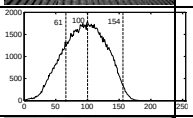	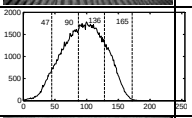	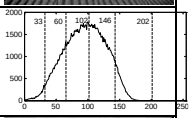
Pyramid	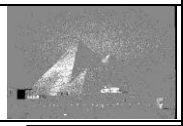	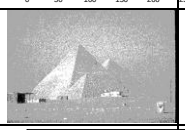	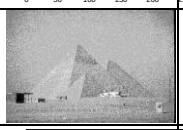	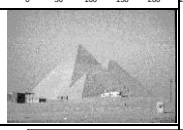
	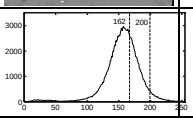	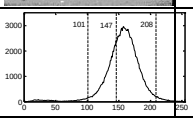	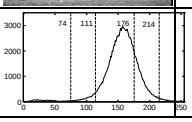	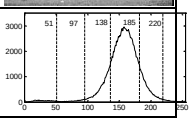

Table 9. Image quality measure values for PN stained image

	T	NAE			NCC			AD			SC		
		FDPSO	BA	FA	FDPSO	BA	FA	FDPSO	BA	FA	FDPSO	BA	FA
Butterfly	2	**0.33±0.01**	0.40±0.01	0.38±0.02	**0.92±0.04**	0.89±0.07	0.88±0.10	**16.68±0.10**	21.39±0.18	19.46±0.12	**1.15±0.03**	1.24±0.10	1.19±0.01
	3	**0.24±0.01**	0.37±0.02	0.30±0.02	**1.01±0.03**	0.94±0.10	0.93±0.05	**10.21±0.05**	17.30±0.20	12.08±0.15	**1.02±0.05**	1.18±0.03	1.14±0.10
	4	**0.16±0.01**	0.31±0.03	0.26±0.03	**1.03±0.11**	0.98±0.10	0.96±0.08	**10.04±0.13**	14.52±0.10	10.75±0.20	**0.94±0.02**	1.03±0.10	1.07±0.02
	5	**0.14±0.02**	0.23±0.03	0.21±0.03	**1.05±0.10**	1.02±0.12	1.00±0.12	**1.29±0.04**	9.06±0.18	5.42±0.22	**0.88±0.01**	1.00±0.10	0.93±0.01
Starfish	2	**0.28±0.02**	0.32±0.01	0.30±0.03	**1.01±0.05**	0.88±0.02	0.88±0.05	**21.42±0.12**	29.18±0.22	26.26±0.12	**1.91±0.05**	1.96±0.01	1.92±0.10
	3	**0.24±0.01**	0.29±0.02	0.27±0.01	**1.02±0.03**	0.90±0.01	0.89±0.06	**17.03±0.15**	23.11±0.08	19.05±0.25	**1.16±0.01**	1.34±0.10	1.27±0.03
	4	**0.20±0.01**	0.27±0.01	0.24±0.01	**1.04±0.02**	0.95±0.05	0.93±0.02	**14.45±0.10**	18.73±0.05	16.54±0.02	**1.12±0.02**	1.17±0.03	1.18±0.10
	5	**0.14±0.01**	0.21±0.01	0.19±0.01	**1.05±0.01**	0.97±0.01	0.98±0.01	**7.22±0.10**	12.06±0.10	10.63±0.12	**1.01±0.02**	1.08±0.01	1.05±0.02
Snake	2	**0.28±0.01**	0.32±0.03	0.34±0.01	**0.91±0.01**	0.88±0.02	0.89±0.03	**22.13±0.10**	34.16±0.01	26.97±0.10	**1.94±0.01**	2.12±0.16	1.98±0.15
	3	**0.25±0.01**	0.29±0.02	0.29±0.02	**0.98±0.01**	0.95±0.02	0.94±0.01	**21.57±0.12**	29.05±0.16	24.00±0.20	**1.38±0.01**	1.97±0.10	1.72±0.03
	4	**0.22±0.01**	0.27±0.03	0.25±0.01	**1.04±0.05**	1.02±0.01	1.00±0.01	**19.54±0.15**	22.46±0.02	21.36±0.20	**1.32±0.05**	1.64±0.03	1.61±0.01
	5	**0.14±0.01**	0.21±0.01	0.22±0.01	**1.06±0.01**	1.05±0.10	1.04±0.02	**8.71±0.02**	16.85±0.12	16.48±0.12	**1.04±0.01**	1.32±0.11	1.27±0.01
Jet	2	**0.28±0.01**	0.35±0.01	0.34±0.03	**0.85±0.02**	0.84±0.01	0.84±0.01	**22.19±0.01**	28.10±0.01	27.03±0.02	**1.25±0.02**	1.64±0.01	1.55±0.10
	3	**0.21±0.01**	0.31±0.03	0.29±0.01	**0.89±0.02**	0.87±0.10	0.86±0.07	**17.15±0.01**	22.42±0.02	20.16±0.02	**1.04±0.02**	1.22±0.11	1.37±0.02
	4	**0.16±0.01**	0.25±0.02	0.27±0.02	**0.93±0.01**	0.91±0.01	0.92±0.01	**14.11±0.01**	19.36±0.10	18.58±0.02	**0.98±0.02**	1.01±0.02	1.11±0.12
	5	**0.14±0.02**	0.23±0.01	0.20±0.01	**0.96±0.01**	0.94±0.01	0.94±0.05	**2.85±0.01**	10.15±0.11	6.49±0.02	**0.96±0.01**	0.99±0.01	0.98±0.02
Desert	2	**0.41±0.01**	0.52±0.03	0.48±0.03	**0.85±0.08**	0.83±0.10	0.84±0.14	**14.10±0.02**	27.14±0.20	19.42±0.12	**1.03±0.01**	1.18±0.05	1.20±0.03
	3	**0.34±0.01**	0.47±0.01	0.43±0.01	**0.88±0.01**	0.86±0.01	0.86±0.01	**10.86±0.01**	23.09±0.01	14.88±0.02	**1.01±0.01**	1.13±0.03	1.16±0.10
	4	**0.28±0.01**	0.40±0.01	0.36±0.01	**0.93±0.03**	0.91±0.06	0.90±0.15	**6.18±0.02**	16.14±0.02	9.37±0.12	**1.00±0.05**	1.05±0.01	1.10±0.02
	5	**0.25±0.01**	0.32±0.03	0.33±0.02	**1.01±0.01**	0.98±0.01	0.99±0.01	**1.05±0.02**	8.56±0.12	6.04±0.02	**0.96±0.01**	1.02±0.01	1.05±0.03
Pyramid	2	**0.39±0.01**	0.46±0.01	0.44±0.01	**0.86±0.02**	0.84±0.11	0.84±0.06	**37.18±0.01**	42.00±0.10	40.75±0.11	**1.00±0.02**	1.13±0.10	1.08±0.01
	3	**0.35±0.01**	0.41±0.01	0.40±0.01	**0.94±0.01**	0.93±0.06	0.93±0.03	**29.05±0.01**	36.74±0.01	33.18±0.20	**0.95±0.01**	1.04±0.02	1.03±0.09
	4	**0.28±0.01**	0.32±0.03	0.34±0.02	**0.97±0.03**	0.95±0.01	0.96±0.05	**11.18±0.02**	22.16±0.12	16.22±0.08	**0.92±0.02**	1.01±0.10	0.98±0.10
	5	**0.25±0.01**	0.27±0.01	0.32±0.01	**0.98±0.01**	0.96±0.03	0.97±0.04	**8.62±0.01**	16.84±0.01	11.47±0.12	**0.90±0.01**	0.94±0.10	0.93±0.12
Average		**0.25±0.01**	0.33±0.02	2.29±0.02	**0.97±0.03**	0.93±0.05	0.92±0.05	**14.37±0.06**	21.69±0.09	18.02±0.11	**1.12±0.02**	1.27±0.07	1.24±0.47

Table 10. Comparison of CPU time, PSNR and MSSIM for GN stained dataset

	T	CPU time (s)			PSNR(dB)			MSSIM		
		FDPSO	BA	FA	FDPSO	BA	FA	FDPSO	BA	FA
Butterfly	2	11.37±0.12	11.28±0.10	**10.85**±0.02	**12.79±0.01**	12.45±0.10	12.12±0.01	**0.55±0.02**	0.53±0.06	0.52±0.03
	3	**15.38±0.10**	18.00±0.12	16.47±0.10	**13.29±0.01**	12.67±0.12	12.33±0.14	**0.57±0.07**	0.56±0.10	0.56±0.01
	4	21.61±0.09	**20.53±0.15**	20.81±0.01	**14.94±0.10**	13.00±0.02	13.62±0.02	**0.66±0.01**	0.60±0.01	0.61±0.05
	5	**24.04±0.02**	24.85±0.20	25.30±0.06	**15.05±0.02**	14.26±0.01	14.32±0.10	**0.68±0.02**	0.62±0.01	0.64±0.02
Starfish	2	**11.24±0.01**	13.16±0.15	12.54±0.07	**11.83±0.02**	11.47±0.05	11.05±0.01	**0.45±0.01**	0.42±0.01	0.44±0.01
	3	**15.31±0.11**	16.83±0.05	17.00±0.15	**12.40±0.01**	11.58±0.01	11.21±0.12	**0.50±0.01**	0.49±0.01	0.46±0.02
	4	**19.57±0.02**	20.04±0.10	20.75±0.11	**13.87±0.10**	12.11±0.02	12.24±0.10	**0.59±0.05**	0.54±0.10	0.55±0.02
	5	24.00±0.10	**23.84±0.12**	24.12±0.10	**14.40±0.02**	13.49±0.10	13.14±0.15	**0.63±0.02**	0.62±0.12	0.62±0.11
Snake	2	**8.59±0.05**	11.62±0.08	10.04±0.15	**10.26±0.02**	9.31±0.01	9.31±0.10	**0.49±0.03**	0.47±0.08	0.48±0.05
	3	13.18±0.02	14.10±0.10	**12.73±0.01**	**11.72±0.02**	10.70±0.02	10.84±0.11	**0.61±0.01**	0.57±0.06	0.54±0.02
	4	**14.96±0.04**	16.27±0.02	17.05±0.12	**13.75±0.10**	11.95±0.05	13.17±0.02	**0.73±0.01**	0.70±0.05	0.71±0.02
	5	**17.74±0.10**	18.44±0.04	19.38±0.15	**16.27±0.01**	14.32±0.10	15.08±0.13	**0.82±0.01**	0.76±0.05	0.75±0.01
Jet	2	**7.19±0.10**	9.39±0.10	8.86±0.10	**10.66±0.11**	10.27±0.02	10.50±0.10	**0.49±0.06**	0.45±0.01	0.43±0.14
	3	**10.52±0.02**	11.74±0.02	12.28±0.10	**12.19±0.05**	10.84±0.02	11.09±0.10	**0.58±0.02**	0.53±0.02	0.56±0.05
	4	17.66±0.01	17.22±0.04	**16.26±0.01**	**13.71±0.04**	11.85±0.01	11.93±0.01	**0.70±0.01**	0.69±0.02	0.64±0.02
	5	**19.52±0.02**	21.97±0.10	22.18±0.15	**15.37±0.02**	12.71±0.05	14.66±0.10	**0.73±0.01**	0.72±0.09	0.69±0.02
Desert	2	**9.94±0.10**	13.15±0.10	10.33±0.10	**9.51±0.10**	8.26±0.01	8.38±0.10	**0.47±0.02**	0.44±0.06	0.46±0.02
	3	16.17±0.10	17.20±0.01	**15.29±0.02**	**11.61±0.01**	9.83±0.02	11.00±0.02	**0.48±0.04**	0.46±0.01	0.48±0.01
	4	**20.85±0.01**	21.28±0.02	22.36±0.15	**13.49±0.01**	12.35±0.05	12.56±0.16	**0.64±0.01**	0.60±0.05	0.63±0.02
	5	**23.32±0.10**	26.93±0.01	24.05±0.10	**14.30±0.01**	13.60±0.01	13.29±0.01	**0.71±0.01**	0.68±0.05	0.70±0.13
Pyramid	2	**8.94±0.02**	9.13±0.10	11.28±0.10	**13.58±0.02**	11.98±0.01	13.10±0.10	**0.52±0.01**	0.52±0.01	0.51±0.07
	3	**12.26±0.02**	16.33±0.10	15.88±0.10	**14.36±0.14**	12.29±0.05	14.15±0.02	**0.65±0.02**	0.63±0.06	0.64±0.04
	4	19.88±0.01	**19.00±0.01**	19.25±0.10	**16.03±0.01**	12.86±0.10	15.62±0.10	**0.73±0.02**	0.73±0.10	0.72±0.01
	5	**21.75±0.10**	21.84±0.10	23.52±0.05	**16.77±0.02**	13.95±0.05	16.32±0.02	**0.81±0.01**	0.79±0.04	0.79±0.06
Average		**16.04±0.06**	17.26±0.08	17.02±0.09	**13.42±0.04**	12.00±0.46	12.54±0.08	**0.62±0.02**	0.59±0.05	0.59±0.04

Table 11. Thresholded images and optimal threshold values for GN stained dataset

	T=2	*T*=3	*T*=4	*T*=5
Butterfly	 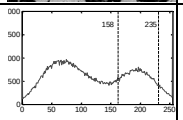	 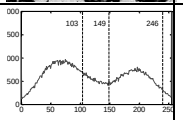	 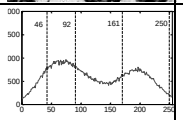	 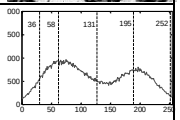
Starfish	 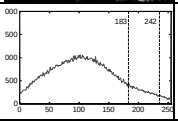	 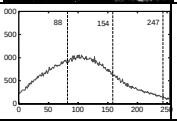	 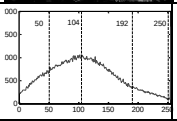	 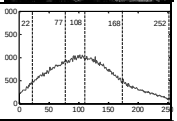
Snake	 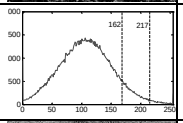	 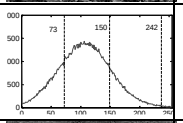	 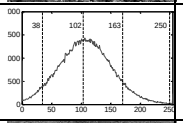	 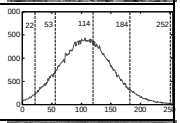
Jet	 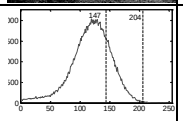	 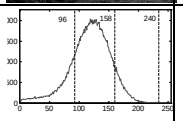	 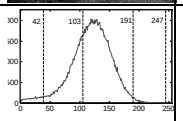	 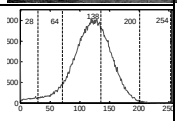
Desert	 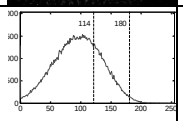	 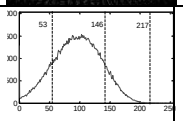	 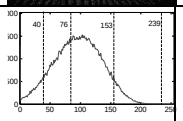	 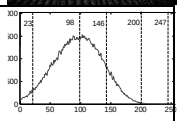
Pyramid	 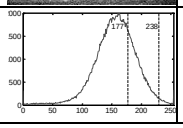	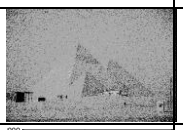 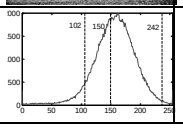	 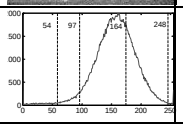	 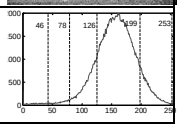

Retrieval Number: K15260981119/19©BEIESP
DOI: 10.35940/ijitee.K1520.0981119
Journal Website: www.ijitee.org

Published By:
Blue Eyes Intelligence Engineering
and Sciences Publication (BEIESP)

Table 12. Image quality measure values for GN stained dataset

	T	NAE			NCC			AD			SC		
		FDPSO	BA	FA	FDPSO	BA	FA	FDPSO	BA	FA	FDPSO	BA	FA
Butterfly	2	**0.43±0.01**	0.50±0.02	0.46±0.01	**0.76±0.05**	0.68±0.06	0.75±0.10	**40.47±0.12**	44.93±0.15	41.04±0.10	**1.28±0.06**	1.58±0.12	1.33±0.05
	3	**0.39±0.01**	0.47±0.02	0.41±0.01	**0.89±0.01**	0.74±0.09	0.84±0.08	**28.39±0.05**	33.02±0.10	30.00±0.16	**1.01±0.02**	1.41±0.06	1.17±0.12
	4	**0.31±0.02**	0.43±0.02	0.38±0.02	**0.96±0.03**	0.82±0.12	0.89±0.01	**16.50±0.03**	26.18±0.12	22.12±0.11	**0.93±0.01**	1.05±0.02	0.96±0.11
	5	**0.30±0.02**	0.35±0.01	0.34±0.02	**0.99±0.02**	0.89±0.01	0.94±0.02	**5.99±0.12**	10.17±0.09	8.52±0.05	**0.87±0.01**	0.92±0.02	0.90±0.05
Starfish	2	**0.55±0.01**	0.57±0.01	0.55±0.02	**0.74±0.01**	0.70±0.02	0.69±0.04	**37.59±0.02**	38.29±0.08	41.44±0.18	**1.34±0.01**	1.76±0.01	1.48±0.01
	3	**0.48±0.01**	0.52±0.02	0.53±0.02	**0.81±0.01**	0.74±0.02	0.76±0.02	**33.07±0.02**	34.10±0.05	36.27±0.04	**1.15±0.02**	1.49±0.13	1.21±0.02
	4	**0.39±0.02**	0.50±0.02	0.43±0.01	**0.86±0.02**	0.82±0.01	0.84±0.05	**25.36±0.10**	27.18±0.01	28.40±0.11	**1.11±0.15**	1.31±0.01	1.16±0.01
	5	**0.36±0.02**	0.38±0.01	0.40±0.01	**0.91±0.02**	0.88±0.10	0.90±0.14	**18.19±0.11**	20.06±0.11	21.37±0.07	**1.03±0.07**	1.16±0.14	1.08±0.10
Snake	2	**0.74±0.02**	0.81±0.01	0.78±0.02	**0.54±0.01**	0.52±0.11	0.48±0.11	**51.17±0.10**	54.29±0.10	59.41±0.03	**1.96±0.02**	2.04±0.11	2.27±0.19
	3	**0.52±0.01**	0.68±0.01	0.61±0.02	**0.67±0.08**	0.63±0.02	0.65±0.02	**43.21±0.01**	48.33±0.22	50.04±0.02	**1.46±0.02**	1.60±0.06	1.83±0.05
	4	**0.41±0.01**	0.50±0.02	0.52±0.02	**0.82±0.01**	0.71±0.03	0.80±0.10	**29.21±0.01**	32.05±0.01	42.62±0.15	**1.27±0.01**	1.52±0.01	1.63±0.05
	5	**0.29±0.01**	0.44±0.02	0.33±0.02	**0.97±0.04**	0.87±0.05	0.88±0.02	**6.01±0.02**	13.95±0.01	28.16±0.01	**0.94±0.05**	1.18±0.10	1.14±0.01
Jet	2	**0.51±0.02**	0.61±0.02	0.53±0.02	**0.64±0.02**	0.58±0.02	0.62±0.02	**42.37±0.12**	46.18±0.10	43.33±0.03	**1.82±0.01**	2.27±0.01	2.06±0.01
	3	**0.41±0.02**	0.56±0.02	0.49±0.02	**0.67±0.02**	0.65±0.02	0.64±0.10	**40.40±0.02**	42.00±0.01	41.85±0.10	**1.62±0.01**	1.94±0.05	1.85±0.07
	4	**0.36±0.02**	0.45±0.01	0.41±0.01	**0.82±0.10**	0.73±0.09	0.78±0.10	**22.73±0.02**	36.82±0.01	37.05±0.02	**1.19±0.01**	1.55±0.01	1.33±0.01
	5	**0.27±0.02**	0.38±0.01	0.33±0.02	**0.85±0.01**	0.80±0.05	0.83±0.09	**19.19±0.02**	23.85±0.15	26.12±0.09	**1.11±0.03**	1.46±0.03	1.20±0.11
Desert	2	**0.74±0.01**	0.88±0.02	0.91±0.02	**0.76±0.10**	0.74±0.05	0.74±0.05	**26.85±0.10**	33.91±0.10	28.19±0.01	**1.16±0.11**	1.20±0.01	1.33±0.10
	3	**0.58±0.01**	0.73±0.02	0.61±0.02	**0.81±0.01**	0.77±0.02	0.80±0.10	**23.73±0.01**	26.14±0.07	26.53±0.05	**1.36±0.01**	1.17±0.01	1.25±0.10
	4	**0.47±0.01**	0.47±0.02	0.53±0.01	**0.84±0.02**	0.80±0.02	0.82±0.10	**20.80±0.02**	23.19±0.02	21.17±0.15	**0.97±0.01**	1.16±0.08	1.19±0.15
	5	**0.42±0.02**	0.43±0.01	0.48±0.02	**0.87±0.01**	0.83±0.01	0.84±0.01	**18.25±0.06**	20.85±0.10	18.46±0.12	**0.91±0.01**	1.12±0.06	1.14±0.02
Pyramid	2	**0.32±0.02**	0.48±0.01	0.37±0.02	**0.90±0.02**	0.88±0.10	0.89±0.01	**17.00±0.10**	21.07±0.12	22.16±0.10	**1.06±0.02**	1.31±0.01	1.23±0.10
	3	**0.29±0.01**	0.32±0.02	0.31±0.01	**0.96±0.05**	0.93±0.02	0.95±0.05	**6.66±0.07**	15.52±0.11	17.84±0.02	**0.98±0.02**	1.28±0.18	1.15±0.01
	4	**0.23±0.01**	0.30±0.01	0.26±0.02	**0.98±0.02**	0.96±0.01	0.96±0.02	**6.87±0.01**	11.83±0.01	11.00±0.12	**0.97±0.01**	1.22±0.11	1.10±0.10
	5	**0.18±0.02**	0.25±0.01	0.22±0.02	**0.99±0.06**	0.98±0.10	0.98±0.01	**1.52±0.10**	5.11±0.08	8.23±0.10	**0.95±0.01**	1.16±0.02	1.03±0.06
Average		**0.41±0.02**	0.50±0.02	0.47±0.02	**0.83±0.03**	0.78±0.05	0.80±0.06	**24.23±0.06**	28.71±0.08	29.64±0.08	**1.19±0.03**	1.41±0.06	1.33±0.07

Table 13. Maximized *f(T)* for images with and without noise

	T	Tsallis function								
		Original image			Image with PN			Image with GN		
		FDPSO	BA	FA	FDPSO	BA	FA	FDPSO	BA	FA
Butterfly	2	**1.0376**	1.0113	1.0094	**1.1187**	1.0073	1.0028	**1.1063**	1.0967	0.8352
	3	**1.2847**	1.2108	1.1948	**1.3316**	1.2774	1.1746	**1.7304**	1.6482	1.3184
	4	**1.4926**	1.2985	1.2792	**1.5104**	1.3116	1.3380	**1.9003**	1.7353	1.8241
	5	**1.6866**	1.4398	1.5023	**1.6772**	1.4405	1.3965	**2.4185**	2.0114	2.2006
Starfish	2	**0.9736**	0.9714	0.9720	**1.1863**	1.0582	1.1593	**0.9377**	0.8503	0.9286
	3	**1.4291**	1.4236	1.4284	**1.2904**	1.1104	1.1806	**1.3183**	1.1942	1.2004
	4	**1.6318**	1.6292	1.6295	**1.5527**	1.3085	1.3824	**1.6824**	1.5538	1.4927
	5	**1.6972**	1.6916	1.6956	**1.5926**	1.4662	1.4757	**1.9930**	1.8642	1.8924
Snake	2	**1.1416**	1.1310	1.1393	**1.2874**	1.1836	1.0946	**1.0642**	0.9517	0.9915
	3	**1.5879**	1.5755	1.5861	**1.3771**	1.2646	1.1977	**1.2773**	1.0843	1.1406
	4	**1.6092**	1.6081	1.5932	**1.5280**	1.3084	1.3005	**1.5825**	1.3382	1.5117
	5	**1.7926**	1.7901	1.7890	**1.6392**	1.5743	1.4853	**1.7249**	1.6200	1.7036
Jet	2	**1.1204**	1.1101	1.1187	**1.0937**	1.0852	0.9847	**0.9365**	0.9226	0.8418
	3	**1.2851**	1.2812	1.2849	**1.2283**	1.1506	1.0388	**1.1582**	1.0578	1.0063
	4	**1.4072**	1.4017	1.4064	**1.4298**	1.3392	1.2250	**1.5007**	1.3994	1.4932
	5	**1.6974**	1.6949	1.6901	**1.5336**	1.3816	1.2974	**1.6255**	1.5030	1.5517
Desert	2	**0.9165**	0.8824	0.9076	**1.1137**	1.0054	1.0279	**1.0457**	0.9747	1.0173
	3	**1.2902**	1.2581	1.2803	**1.2903**	1.1528	1.1048	**1.4883**	1.2735	1.3306
	4	**1.4111**	1.4074	1.4085	**1.4284**	1.2005	1.2881	**1.8280**	1.6504	1.7399
	5	**1.9977**	1.8753	1.9025	**1.5118**	1.3746	1.4642	**2.0056**	1.8372	1.9362
Pyramid	2	**0.9063**	0.8774	0.8983	**1.0046**	0.9946	0.9859	**0.9925**	0.9767	0.9813
	3	**1.3792**	1.1965	1.3100	**1.2794**	1.0472	1.0437	**1.1694**	1.0045	1.1629
	4	**1.5005**	1.4723	1.3972	**1.4007**	1.2952	1.2811	**1.6382**	1.4826	1.5992
	5	**1.7824**	1.7107	1.5773	**1.5225**	1.3379	1.3837	**1.9245**	1.6202	1.8114

Once again, regardless on the number of thresholds and noise added to the images, the FDPSO clearly shows a superior performance when compared to BA and FA. Table 13 presents a general overview of the results obtained with and without noisy images.

In the literature, several statistical procedures, such as ANOVA [5, 6], Kruskal-Wallis [50], etc., are available to compute statistical significant differences between methods. In the proposed work, the Wilcoxon's rank test [47, 48] is taken for the process of image segmentation. It is a non-parametric approach, generally considered to evaluate result variation among two associated procedures. This rank test is initially executed with MSSIM and later extended for *f(T)* and PSNR by considering a 5% significance level related to the chosen *T* value with 40 independent samples. This test is performed for the clear and noisy image dataset and the corresponding *p*-value obtained for MSSIM with FDPSO vs.BA and FDPSO vs. FA are presented in Table 14. The *p*-values presented in this table are very less compared with 0.05 (5% significance level), which confirms the FDPSO's search ability against the null hypothesis. These results confirm the search ability of FDPSO over BA and FA. Similar results are obtained with Wilcoxon's test for *f(T)* and PSNR with the considered image dataset.

Table 14. Wilcoxon's grade value for clear and noisy images

	T	*p*- Value					
		Original image		Image with PN		Image with GN	
		FDPSO vs. BA	FDPSO vs. FA	FDPSO vs. BA	FDPSO vs. FA	FDPSO vs. BA	FDPSO vs. FA
Butterfly	2	3.1094 E-05	2.1194 E-07	5.1038 E-08	3.2910 E-06	1.2993 E-04	1.1937 E-06
	3	1.2295 E-04	4.9375 E-07	2.4875 E-06	2.6645 E-07	2.0045 E-07	1.0746 E-07
	4	2.0165 E-7	1.1186 E-06	3.2928 E-06	1.1163 E-06	1.3838 E-08	2.0084 E-05
	5	1.2828 E-07	1.0526 E-09	1.3984 E-06	2.1084 E-05	1.6274 E-05	1.1153 E-05
Starfish	2	5.1091 E-08	3.1948 E-05	1.9326 E-08	5.1167 E-09	1.7495 E-05	1.0037 E-05
	3	3.1093 E-10	4.1050 E-06	4.2928 E-07	7.7453 E-07	1.1938 E-07	1.0001 E-06
	4	1.1883 E-06	2.6618 E-06	2.4149 E-05	3.1911 E-06	3.2993 E-07	4.2298 E-07
	5	2.1128 E-05	1.0452 E-08	1.3774 E-10	5.2293 E-08	7.1170 E-06	2.0015 E-04
Snake	2	8.1226 E-08	1.0006 E-09	5.9493 E-06	1.9936 E-06	1.1046 E-05	1.1937 E-04
	3	6.2495 E-06	2.2800 E-07	1.0047 E-07	4.0045 E-08	1.1038 E-08	2.1874 E-09
	4	2.1185E-07	1.1145 E-07	3.3305 E-07	2.1936 E-09	5.2837 E-06	1.1888 E-06
	5	1.3363 E-13	1.8266 E-08	6.2274 E-04	4.4401 E-05	2.1916 E-08	4.7353 E-06
Jet	2	3.1153 E-06	1.0095 E-06	2.1194 E-05	6.1836 E-06	1.0047 E-06	5.0026 E-08
	3	8.0027 E-10	1.1171 E-05	5.2211 E-05	4.2287 E-06	1.3745 E-05	1.1038 E-07
	4	4.1953 E-07	2.0527 E-10	4.1927 E-08	1.1934 E-10	1.8488 E-07	1.1114 E-05
	5	2.2257 E-06	1.8342 E-06	2.3387 E-06	1.3938 E-08	7.1176 E-07	5.8221 E-05
Desert	2	1.8462 E-12	3.9194 E-08	5.0026 E-04	4.1187 E-07	4.2085 E-06	3.2874 E-05
	3	4.1163 E-06	2.1148 E-06	2.2847 E-06	7.1736 E-08	1.1037 E-08	7.1732 E-07
	4	2.1046 E-08	1.9964 E-06	3.3319 E-05	9.1383 E-06	3.3827 E-07	1.1183 E-09
	5	1.2202 E-07	1.4265 E-07	1.1038 E-05	2.1984 E-05	2.0009 E-08	2.9945 E-06
Pyramid	2	4.0037 E-11	2.8634 E-09	2.3845 E-05	5.2294 E-07	1.1028 E-06	1.1517 E-06
	3	3.3375 E-06	1.0007 E-07	1.1124 E-07	3.1100 E-08	5.2843 E-09	1.0036 E-08
	4	2.1939 E-06	1.3003 E-11	3.3352 E-08	1.0057 E-06	6.6027 E-05	6.3135 E-06
	5	2.2800 E-07	1.9437 E-09	2.1093 E-04	2.5518 E-05	1.1114 E-07	2.2814 -06

VI. CONCLUSION

In this paper, a multi-level thresholding is presented for gray scale image dataset using FDPSO and Tsallis function. This procedure finds the optimal threshold for a chosen image with a chosen *T* value. The proposed segmentation technique is compared with other heuristic algorithms, such as BA and FA. The performance of FDPSO is evaluated using quantitative and qualitative measures, such as *f(T)*, CPU time, STD, PSNR, MSSIM, NAE, NCC, AD and SC. The robustness of the segmentation scheme is verified by considering PN and GN corrupted image dataset. The experimental results confirm that the FDPSO assisted segmentation procedure offers better results in most of the cases when compared with BA and FA. Wilcoxon's rank test also proves that, FDPSO based image segmentation process is statistically superior in both the clear and noisy image dataset.

REFERENCES

1. Ghamisi, P., Couceiro, M. S. and Benediktsson, J.A,. "Extending the fractional order Darwinian particle swarm optimization to segmentation of hyperspectral images," SPIE Remote Sensing, 85370F-85370F-11(2012).
2. Ghamisi, P., Couceiro, M. S., Benediktsson, J. A. and Ferreira, N. M. F,. "An efficient method for segmentation of images based on fractional calculus and natural selection," Expert Syst. Appl., vol.39, no.16, pp.12407– 12417(2012).

3. Ghamisi, P., Couceiro, M. S. and Benediktsson, J.A,.“Classification of hyperspectral images with binary fractional order Darwinian PSO and random forests,” SPIE Remote Sensing, 88920S-88920S-8(2013).
4. Ghamisi, P., Couceiro, M. S., Martins, F. M. L. and Benediktsson, J. A,.. “Multilevel image segmentation based on fractional-order Darwinian particle swarm optimization,” IEEE Transaction on Geoscience and Remote sensing, vol.52, no.5, pp. 2382-2394(2014).
5. Manickavasagam, K., Sutha, S. and Kamalanand, K,. “An automated system based on 2d empirical mode decomposition and k-means clustering for classification of Plasmodium species in thin blood smear images,” BMC Infectious Diseases, vol. 14, no. Suppl 3, pp. P13, 2014. doi: 10.1186/1471-2334-14-S3-P13(2014).
6. Manickavasagam, K., Sutha, S. and Kamalanand, K,. “Development of Systems for Classification of Different Plasmodium Species in Thin Blood Smear Microscopic Images,” Journal of Advanced Microscopy Research, vol.9, no.2, pp. 86-92(2014).
7. Cuevas, E., Oliva, D., Díaz, M., Zaldivar, D., Pérez-Cisneros, M. andPajares, G,.”White Blood Cell Segmentation by Circle Detection Using Electromagnetism-Like Optimization,” Computational and Mathematical Methods in Medicine, vol. 2013, Article ID 395071, 15 pages. Doi:10.1155/2013/395071 (2013).
8. Amin, K. M., AbdElfattah, M., Hassanien, A. E., & Schaefer, G,. “A binarization algorithm for historical arabic manuscript images using a neutrosophic approach,” In 9th International Conference on Computer Engineering & Systems (ICCES), IEEE, pp. 266-270. doi: 10.1109/ICCES.2014.7030970 (2014).
9. Oliva, D., Cuevas, E., Pajares, G., Zaldivar, D. andPerez-Cisneros, M,. “Multilevel Thresholding Segmentation Based on Harmony Search Optimization,” Journal of Applied Mathematics, vol. 2013, Article ID 575414, 24 pages. Doi:10.1155/2013/575414 (2013).
10. Oliva, D., Cuevas, E., Pajares, G., Zaldivar, D. andOsuna, V,. “A Multilevel Thresholding algorithm using electromagnetism optimization,” Journal of Neuro Computing, vol. 139, pp. 357-381(2014).
11. Sezgin, M. and Sankar, B,. “Survey over image thresholding techniques and quantitative performance evaluation,” Journal of Electronic Imaging, vol.13, no.1, pp. 146 – 165(2004).
12. Bhattacharyya, S,. “A brief survey of color image preprocessing and segmentation techniques,” Journal of Pattern Recognition Research, vol.1, no.1, pp. 120-129(2011).
13. Tuba, M,. “Multilevel image thresholding by nature-inspired algorithms: A short review,” Computer Science Journal of Moldova, vol.22, no.3, pp. 318-338(2014).
14. Alihodzic, A. and Tuba, M,.”Improved Bat Algorithm Applied to Multilevel Image Thresholding,” The Scientific World Journal, vol.14, Article ID 176718, 16 pages, (2014).
15. Tuba, M. and Brajevic, I., “Modified seeker optimization algorithm for image segmentation by multilevel thresholding,” International Journal of Mathematical Models and Methods in Applied Sciences, vol.7, no.1, pp. 370-378(2013).
16. Bhattacharyya, S., Maulik, U. and Dutta, P., “ Multilevel image segmentation with adaptive image context based thresholding,” Applied Soft Computing, vol.11, no.1, pp. 946-962(2011).
17. Rajinikanth, V. and Couceiro, M.S., “Optimal Multilevel Image Threshold Selection Using a Novel Objective Function, Information Systems Design and Intelligent Applications, Advances in Intelligent Systems and Computing, vol. 340, pp 177-186. Doi: 10.1007/978-81-322-2247-7_19(2015).
18. Raja, N.S.M., Rajinikanth, V. and Latha, K., “Otsu Based Optimal Multilevel Image Thresholding Using Firefly Algorithm,” Journal of Modelling and Simulation in Engineering, vol. 20, Article ID 794574, 17 pages. Doi:10.1155/2014/794574(2014).
19. Sarkar, S. and Das, S., “Multilevel Image Thresholding Based on 2D Histogram and Maximum Tsallis Entropy – A Differential Evolution Approach,” IEEE Transactions on Image Processing, vol.22, no.12, pp.4788-4797(2013).
20. Rajinikanth, V. and Couceiro, M.S., “RGB Histogram Based Color Image Segmentation Using Firefly Algorithm,” Procedia Computer Science, vol. 46, pp. 1449 – 1457. Doi:10.1016/j.procs.2015.02.064(2015).
21. Tsallis, C., “Possible generalization of Boltzmann-Gibbs statistics,” Journal of Statistical Physics, Vol.52, No. 1-2, pp 479-487(1988).
22. Tsallis, C., “Entropic nonextensivity: a possible measure of complexity,” Chaos, Solitons & Fractals, vol.13, no.3, pp. 371-391(2002).
23. Tsallis, C., Anteneodo, C., Borland, L. and Osorio, R., “Nonextensive statistical mechanics and economics,” Physica A: Statistical Mechanics and its Applications, vol.324, no.1, pp. 89-100(2003).
24. Manikantan, K., Arun, B. V. and Yaradonic, D.K.S., “Optimal Multilevel Thresholds based on Tsallis Entropy Method using Golden Ratio Particle Swarm Optimization for Improved Image Segmentation,” Procedia Engineering, vol. 30, pp.364 – 371. Doi:10.1016/j.proeng.2012.01.873(2012).
25. Raja, N. S. M., Kavitha, N. and Ramakrishnan, S. Analysis of vasculature in human retinal images using particle swarm optimization based Tsallis multi-level thresholding and similarity measures, Lecture Notes in Computer Science, Volume 7677, pp. 380-387. Doi: 10.1007/978-3-642-35380-2_45(2012).
26. Sathya, P.D. and Kayalvizhi, R.,“PSO-based TsallisThresholding Selection Procedure for Image Segmentation, “International Journal of Computer Applications, vol.5, no. 4, pp. 39–46. Doi: 10.5120/903-1279(2010).
27. Sarkar, S., Das, S. and Chaudhuri, S.S.,”Multilevel Image Thresholding Based on Tsallis Entropy and Differential Evolution,” Swarm, Evolutionary, and Memetic Computing, Notes in Computer Science, Volume 7677,pp 17-24.Doi: 10.1007/978-3-642-35380-2_3(2012).
28. Paul, S. andBandyopadhyay, B., “A novel approach for image compression based on multi-level image thresholding using Shannon Entropy and Differential Evolution,” Students' Technology Symposium (TechSym), IEEE, pp. 56 – 61, Doi: 10.1109/TechSym.2014.6807914(2014).
29. Sarkar,S., Das, S., Paul, S., Polley, S., Burman, R. and Chaudhuri, S.S., “Multi-level image segmentation based on fuzzy-Tsallis entropy and differential evolution,” IEEE International Conference on Fuzzy Systems (FUZZ), pp.1-8, Doi: 10.1109/FUZZ-IEEE.2013.6622406(2013).
30. Sathya, P.D. and Kayalvizhi, R., “Optimum Multilevel Image Thresholding Based on Tsallis Entropy Method with Bacterial Foraging Algorithm,” International Journal of Computer Science Issues, vol. 7. no.5, pp. 336-343(2010).
31. Agrawal, S., Panda, R., Bhuyan, S. and Panigrahi, B.K., “Tsallis entropy based optimal multilevel thresholding using cuckoo search algorithm,” Swarm and Evolutionary Computation, vol.11, pp.16–30(2013).
32. Zhang, Y. and Wu, L., “Optimal Multi-Level Thresholding Based on Maximum Tsallis Entropy via an Artificial Bee Colony Approach, “Entropy, vol. 13, pp. 841-859; Doi:10.3390/e13040841(2011).
33. Bhandari, A.K., Kumar, A. and Singh, G.K., “Modified artificial bee colony based computationally efficient multilevel thresholding for satellite image segmentation using Kapur’s,” Otsu and Tsallis functions”, Expert Systems with Applications, vol. 42, no. 3, pp. 1573–1601(2015).
34. Wang, Z., Bovik, A.C., Sheikh, H. R. and Simoncelli, E.P., “Image Quality Assessment: From Error Visibility to Structural Similarity,” IEEE Transactions on Image Processing, vol. 13, no. 4, pp. 600 – 612(2004).
35. Grgic, S., Grgic, M. and Mrak. M., “Reliability of objective picture quality measures,” Journal of Electrical Engineering, Vol. 55, No. 1-2, pp. 3–10(2004).
36. Ghosh, S.K., Digital Image Processing, Narosa Publishing House Pvt. Ltd., New Delhi(2012).
37. Pires, E.J.S., Machado, J.A.T., Oliveira, P.B.M., Cunha, J.B. and Mendes, L., “Particle swarm optimization with fractional-order velocity,” Journal on Nonlinear Dynamics, vol.61, no.1-2, pp 295-301(2010).
38. Tillett, T., Rao, T.M., Sahin, F. and Rao, R., “Darwinian particle swarm optimization,” Proceedings of the 2nd Indian international conference on artificial intelligence, Pune, Índia, 1474–1487(2005).
39. Couceiro, M.S., Rocha, R.P., Ferreira, N.M.F. and Machado, J.A.T., “Introducing the fractional-order Darwinian PSO,” Signal Image and Video Processing, vol.6, no.3, pp. 343–350(2012).
40. Kennedy, J. and Eberhart, R. C., „Particle swarm optimization.“ In Proceedings of IEEE international conference on neural networks, 1942-1948. doi: 10.1109/ICNN.1995.488968(1995).

41. Couceiro, M. S., Machado, J. T., Rocha, R. P., & Ferreira, N. M., "A fuzzified systematic adjustment of the robotic Darwinian PSO," Robotics and Autonomous Systems, vol.60, no.12, pp. 1625-1639(2012).
42. A.Sheryl Oliver,M.Anuradha.J.Jean Justus, Maheswari N ,"Optimized low computational algorithm for elderly fall detection based on machine learning techniques" Biomedical Research,2018 Volume 29, Issue 20.
43. Yang, X.S. Nature-Inspired Metaheuristic Algorithms, 2nd edition. Luniver Press, Frome, UK(2010).
44. Yang, XS., "A new metaheuristic bat-inspired algorithm. In: Nature Inspired Cooperative Strategies for Optimization (NICSO 2010) (Eds. Cruz C. , Gonzalez J. , Krasnogor N. , and Terraza G.)," Springer, SCI 284, pp 65-74(2010).
45. Yang, X.S., "Bat algorithm: literature review and applications," Int. J. Bio-Inspired Computation, Vol. 5, No. 3, pp. 141–149(2013).
46. Yang, X.S., "Firefly algorithm, stochastic test functions and design optimization," International Journal of Bio-Inspired Computation, vol. 2, no. 2, pp. 78–84(2010).
47. Yang, X.S., "Review of meta-heuristics and generalised evolutionary walk algorithm," International Journal of Bio-Inspired Computation, vol. 3, no. 2, pp. 77–84(2011).
48. A. Sheryl Oliver, Dr. N. Maheshwari, Dr. Andrews Samraj, , " Stable and Critical Gesticulation recognition in children and pregnant women by SVM Classification", Maxwell publications, Research Journal of Applied Sciences of Engineering and Technology,Vol 7, Issue : 23, Pages : 4917 – 4926, Jun 20,2014.
49. A.Sheryl Oliver, Maheshwari.N,(2014)" Pigeon Hole Technique in Optimization of Wearable Electrodes used in Danger and Safety Zone Prediction for Toddlers" International Journal of Applied Engineering Research, ISSN 0973-4562 Volume 9, Number 24 (2014) pp. 25741-25755.
50. A. Sheryl Oliver, N. Maheswari(2016), 'Identifying the Gestures of Toddler, Pregnant Woman and Elderly using Segmented Pigeon hole feature extraction technique and IRthreshold Classifier", Indian Journal of Science and Technology, Vol. 9, Issue.39, pp. 2325-2330 .
51. Martin, D., Fowlkes, C., Tal, D. and Malik, J., "A database of human segmented natural images and its application to evaluating segmentation algorithms and measuring ecological statistics," Technical Report UCB CSD-01-1133, University of California at Berkeley. http://http.cs.berkeley.edu/projects/vision/Grouping/overview.html(2000).
52. Kruskal, W.H. and Wallis, W.A., "Use of Ranks in One-Criterion Variance Analysis," Journal of the American Statistical Association, vol. 47, no. 260, pp. 583-621(1952).
53. García, S., Molina, D., Lozano, M. and Herrera, F., "A Study on the use of nonparametric tests for analyzing the evolutionary algorithms' behaviour: A case study on the CEC 2005 special session on real parameter optimization," Journal of Heuristics, vol.15, pp. 617–644(2009).
54. Oliva, D., Osuna-Enciso, V., Cuevas, E., Pajares, G., Pérez-Cisneros, M. and Zaldívar, D., "Improving segmentation velocity using an evolutionary method," Expert Systems with Applications, vol. 42, pp.5874–5886(2015).

AUTHORS PROFILE

Author-1 Photo

Dr.R.Pugalenthi received the B.E. Degree from Bharathidasan University, Trichy, India in 1999, and the M.E Degree from Sathyabama University, Chennai, India in 2002, and the Ph.D Degree in Data Communication and Networking from Anna University, Chennai, India in 2015. He is currently working as Associate Professor in the Department of Computer Science and Engineering at St.Joseph's College of Engineering, Chennai-600119. His research interests include Image Processing, Mobile Ad Hoc, Wireless Sensor Networks and Network Security..

Author-2 Photo

A.Sheryl Oliver obtained her B.E degree in Computer Science and Engineering from Bharathidasan University.She completed her P.G degree in IASE DU in Information Technology. She pursued her PhD in VIT university, Chennai Campus. Her thesis title is Human Activity Recognition using wearable electrodes. Her area of expertise are Data mining, Machine learning, Wearable computing and Data Science. Currently she is working in St.Joseph's College of Engineering as Associate Professor and has 14 years of experience. Now she is in actively working in Deep Learning and Artificial Intelligence for some real time applications.